Properties of the Kinetochore In Vitro. I. Microtubule Nucleation and Tubulin Binding

T. J. MITCHISON and M. W. KIRSCHNER
Department of Biochemistry, University of California, San Francisco, California 94143

ABSTRACT We have isolated chromosomes from Chinese hamster ovary cells arrested in mitosis with vinblastine and examined the interactions of their kinetochores with purified tubulin in vitro. The kinetochores nucleate microtubule (MT) growth with complex kinetics. After an initial lag phase, MTs are continuously nucleated with both plus and minus ends distally localized. This mixed polarity seems inconsistent with the formation of an ordered, homopolar kinetochore fiber in vivo. As isolated from vinblastine-arrested cells, kinetochores contain no bound tubulin. The kinetochores of chromosomes isolated from colcemid-arrested cells or of chromosomes incubated with tubulin in vitro are brightly stained after anti-tubulin immunofluorescence. This bound tubulin is probably not in the form of MTs. It is localized to the corona region by immunoelectron microscopy, where it may play a role in MT nucleation in vitro.

The kinetochore is a morphologically distinct region of the chromosome that forms at the primary constriction during mitosis (30). In the electron microscope, it often appears as a trilaminar disc, and fibrous material is sometimes seen projecting from the outer, dense layer (15, 32, 34). Several lines of evidence suggest that the kinetochore, by interacting with microtubules (MTs),[1] is responsible for the attachment of the chromosome to the spindle and the subsequent segregation of sister chromatids during anaphase (11, 19, 24). Although it is clear that the kinetochore is designed to interact with MTs, the exact nature of this interaction, as well as its underlying chemistry, is unclear. Electron microscopic studies have shown that the characteristic kinetochore structure generally starts to form in prophase. During prometaphase, after nuclear envelope breakdown in higher eucaryotes, the chromosomes start to interact with the spindle, and MTs are found in the vicinity of the kinetochore. At metaphase, the chromosomes are positioned at the center of the spindle by balanced forces in the direction of the poles (11), and the kinetochore MTs of many species align in parallel to form a well-ordered fiber, terminating in the outer dense layer. Recently, two techniques have been used to demonstrate the structural polarity of mitotic MTs, showing that polar MTs have their plus ends distal to the organizing center, whereas kinetochore fibers have their plus ends proximal to the organizing center (12–14). Such an organization would allow single continuous MTs to run between the pole and the kinetochore, and this type of organization has been found in the simple spindles of some lower eucaryotes in which each kinetochore interacts with a single MT (7, 27, 33). The situation is harder to analyze in larger spindles; at least some kinetochore MTs appear to run directly to the poles in mammalian cells, whereas others may not (6, 8, 29, 40). The evidence from electron microscopy leaves several important questions about spindle formation unresolved: In particular, we wish to know how the connection between the kinetochore and the poles is formed, and how the kinetochore fiber lengthens during prometaphase and shortens during anaphase.

One approach to answering these questions is to study the interaction of the kinetochore with MTs in vitro. The results of such studies have been somewhat confusing. Kinetochores have been shown to nucleate MTs in vitro, when both lysed cells (18, 26, 36) and isolated chromosomes were used (2, 37, 38). The polarity of this interaction has been reported to be a plus end away from the kinetochore in contradiction to the in vivo polarity results (12). Although releasing cells from a drug-induced MT depolymerization demonstrates nucleation at kinetochores in vivo (10, 39), it is not clear whether kinetochores actually nucleate during a normal mitosis (31, 34, 35).

In this and the paper that follows (23), we extend the in vitro observations of kinetochore function in an attempt to

[1] *Abbreviations used in this paper:* CHO, Chinese hamster ovary; MTs, microtubules; PB, 80 mM PIPES, 1 mM EGTA, 1 mM $MgCl_2$, pH 6.8 with KOH.

explain the mechanisms of morphogenesis and resolution of the spindle, and the underlying chemistry of the kinetochore. In this paper, we discuss the interaction of the kinetochore with soluble tubulin and its capacity to nucleate MT growth. In the paper that follows, we describe the interaction of kinetochores with preformed MTs and discuss the dynamics of the MT end at the kinetochore. In both papers, we have attempted to relate in vitro observations to the behavior of the kinetochore during mitosis in vivo, in an effort to elucidate its functional properties.

MATERIALS AND METHODS

Cell Culture and Mitotic Arrest: Wild type Chinese hamster ovary (CHO) cells were provided by Ibrahem Tuet (Cell Culture Facility, University of California at San Francisco). They were maintained in minimum essential α medium with 10% fetal calf serum at 37°C using 7% CO_2 in air, on 150-mm plastic petri dishes. For the routine preparation of mitotic cells, nearly confluent cultures were incubated for 10–12 h in 10 μg/ml of vinblastine sulfate in normal medium. For particular experiments, other drugs were used as noted. Identical results were obtained using synchronization protocols based on a 16-h arrest in 2 mM thymidine, followed by release into fresh medium for 5 h, and then with drug added for 5 h.

Chromosome Isolation: This procedure was developed by modifying the aqueous polyamine method of Lewis and Laemmli (17). Mitotic cells were selectively collected from 10 dishes by squirting a stream of medium over the cells with a pasteur pipette. Cells were pelleted by centrifugation (500 *g*, 2 min) and resuspended in 100 ml of 5 mM NaCl, 5 mM $MgCl_2$, 5 mM PIPES, 0.5 mM EDTA pH 7.2 with KOH. This and all subsequent steps were at 0–4°C. After incubation at 0°C for 10 min to allow swelling, the cells were pelleted again and resuspended in 7 ml of lysis buffer: 10 mM PIPES, 2 mM EDTA, 0.1% β-mercaptoethanol, 1 mM spermidine HCl, 0.5 mM spermine HCl pH 7.2 with KOH. (This concentration of spermine and spermidine is referred to as 2× polyamines). Before use, the buffer was saturated with Digitonin by adding it to 0.1%, stirring at 4°C for 30 min, and spinning out the excess solid. Just before adding it to the cells, α_2 macroglobulin (Boehringer Mannheim Diagnostics, Inc., Houston, TX) was added to 2 μg/ml as a protease inhibitor. The permeabilized cells were transferred to a glass dounce homogenizer and disrupted by ~20 strokes with the tight pestle. After cell disruption, small aliquots of lysate were removed, Hoechst 33258 was added to 2 μg/ml, and then was observed under the fluorescence microscope. When the majority of the spindles were disrupted, the lysate was sedimented at 250 *g* for 1 min to remove debris. The supernatant was layered onto a gradient (total vol 9 ml) in a 15-ml corex tube (Corning Glass Works, Corning, NY) consisting of 20–60% wt/vol sucrose in 10 mM PIPES, 1 mM EDTA, 0.1% β-mercaptoethanol, 1× polyamines pH 7.2 with KOH plus 1 μg/ml of α_2 macroglobulin. The gradient was sedimented at 2,500 *g* for 15 min in a JS-13 (Beckman Instruments, Inc., Palo Alto, CA) swinging bucket rotor. The chromosomes formed a flocculent white mass on the side of the tube at ~50% sucrose. They were collected with a pasteur pipette and used immediately, or frozen in aliquots with liquid nitrogen and stored at −80°C. 10 plates of cells yielded ~10^8 chromosomes in 1 ml.

Other Materials: Phosphocellulose-purified tubulin was used for all experiments. It was purified as described (20) and stored as aliquots at −80°C. CHO centrosomes (20) and axonemes (21) were purified and stored as described. Monoclonal anti-β tubulin was a generous gift of S. Blose (Cold Spring Harbor, NY). Rhodamine and fluorescein goat anti-mouse IgG was from Cappel Laboratories (Cochranville, PA).

Biotinylated Tubulin: Phosphocellulose-purified tubulin was thawed and brought to 33% vol/vol glycerol, 80 mM PIPES, 1 mM EGTA, 6 mM $MgCl_2$, 1 mM GTP, pH 6.8 with KOH (glycerol assembly buffer) at a final concentration of 2–4 mg/ml. MTs were polymerized for 30 min at 37°C. *N*-Hydroxysuccinimidyl biotin (Polysciences, Inc., Warrington, PA) was dissolved at 100 mg/ml in dry dimethyl sulfoxide and added to the MTs, using 4–12 μl reagent/ml MTs. 6 μl/ml gave a derivation level of tubulin with ~2.5 biotins per dimer, which we most often used. However, for the experiments in this paper, we used ~four to five biotins per dimer. To determine the stoichiometry of labeling, we used ^{14}C-labeled *N*-hydroxysuccinimdyl biotin synthesized from [^{14}C]biotin (Amersham Corp., Arlington Heights, IL) as described (14). The MTs were mixed and incubated for 15 min at 37°C with occasional gentle agitation. Monosodium glutamate was added to 10 mM to terminate the reaction, and the MTs were sedimented through 5-ml cushions of 50% wt/vol sucrose in 80 mM PIPES, 1 mM EGTA, 1 mM $MgCl_2$, pH 6.8 with KOH (PB)[2] at 150,000 *g* for 2 h at 37°C in a 50-Ti rotor (Beckman Instruments, Inc.). The supernatant above the sucrose was removed, and the upper surface was washed with PB before the sucrose solution was removed. The pellet was resuspended in PB + 1 mM GTP at 0°C and disrupted with a teflon stirring rod to give a solution of 5–10 mg/ml in tubulin. After incubating for 20 min at 0°C, the solution was sedimented at 150,000 *g* for 20 min at 2°C to remove cold stable aggregates, and the supernatant was brought to the glycerol assembly buffer used in the first polymerization. After polymerizing for 30 min at 37°C, the MTs were sedimented through sucrose as before and were then resuspended and allowed to depolymerize in cold PB + 1 mM GTP as above. After a final cold spin, usually in the airfuge (Beckman Instruments, Inc.) at 90,000 *g* for 10 min at ~8°C, the biotinylated tubulin at 5–10 mg/ml was frozen in aliquots in liquid nitrogen and stored at −80°C. Typically, the yield of protein was ~30% that of the input.

Assay for MT Assembly from Kinetochores: Phosphocellulose-purified tubulin was made up in 1.11× PB + GTP and prewarmed at 37°C for 2 min. Chromosomes were added to give a final buffer of PB + 1 mM GTP containing the appropriate concentration of tubulin and a 10-fold dilution of chromosomes. After incubating at 37°C for an appropriate time, an aliquot of the chromosome suspension was removed and diluted into 10 vol of 1% glutyaraldehyde in PB at 37°C, and then transferred to 25°C. After fixation for at least 3 min at 25°C, the chromosomes were cooled to 0°C. The fixed chromosomes were sedimented through a cushion of 33% vol/vol glycerol in PB onto a polylysine-coated coverslip, using 15-ml corex (Corning Glass Works) tubes modified as described (13). Sedimentation was done at 16,000 *g* for 10 min at 4°C; ~10^5 chromosomes were sedimented onto each 12-mm coverslip. The coverslips were removed, postfixed in methanol at −20°C, and stained by anti-tubulin immunofluorescence as described (20), except that Hoechst 33258 (Sigma Chemical Co., St. Louis, MO) was added to the penultimate phosphate-buffered saline wash at 10 μg/ml to allow visualization of chromatin.

To determine the number of MTs nucleated, we first identified a chromosome by Hoechst staining without previously having looked at the MTs, then under the microscope we counted directly the number of MTs nucleated using the rhodamine filter. 100 chromosomes were counted per coverslip and were averaged. For length measurements, chromosomes were picked at random with the Hoechst filter as above photographed with the rhodamine filter, and digitized as described for centrosomes (20). At least 100 length measurements were made for each time point.

For electron microscopy of nucleation, ~10^6 fixed chromosomes were sedimented onto a coverslip as above and then processed exactly as described for centrosomes (13), except that the tannic acid step was omitted.

Pulse Experiments with Labeled Tubulin: MT polymerization was initiated as above using either axonemes and CHO centrosomes or axonemes and chromosomes, and unlabeled tubulin at 20 μM. The reaction was allowed to proceed for 8 min. Biotinylated tubulin was prewarmed and added to give a final concentration of 25 μM biotinylated tubulin and 10 μM unmodified tubulin. After 10 min at 37°C, the reaction was fixed and sedimented as above. After postfixation in methanol at −20°C for 5 min, the coverslips were rehydrated in 150 mM NaCl, 20 mM Tris, 10 mM NaN_3 pH 7.4 + 1% Triton X-100 + 2 mg/ml of crystalline grade bovine serum albumin (BSA; Sigma Chemical Co.) (TBS + TX + BSA). The coverslips were incubated for 30 min in 3 μg/ml of Texas red–labeled strepavidin (BRL, Bethesda, MD) in TBS + TX + BSA at 25°C. This solution was aspirated and replaced (without washing) with diluted mouse anti-β tubulin in TBS + 0.1% Triton X-100 + 1% BSA (AbDil). After 20 min, the coverslips were washed in TBS + 0.1% Triton X-100 and incubated with fluorescein goat anti-mouse IgG in AbDil for 20 min. The coverslips were then washed in TBS + 0.1% Triton X-100 + 10 μg/ml Hoechst 33258, and mounted in 90% glycerol, 20 mM Tris HCl pH 8. The Texas red label was visualized using the conventional rhodamine isothiocyanate filters, and fields were photographed successively with the fluorescein, rhodamine, and Hoechst filters using Tri-X film (Eastman Kodak Co., Rochester, NY) developed with Diafine. Exposure was typically 20 s for Texas red. For digitizing, the negatives were projected onto paper and the Texas red–labeled segments traced. Then the fluorescein isothiocyanate image was projected, and appropriate labeled segments were measured as described (20).

Tubulin Binding Assay: Chromosomes were incubated in PB + 1 mM GTP with or without 10 μM tubulin for 10 min at 37°C (or other appropriated incubation). They were then diluted to 10^5/ml in PB at 0°C. 1 ml of this solution was sedimented unfixed onto a polylysine coverslip through 33% vol/vol glycerol in PB at 4°C as above. After aspirating the cushion, the coverslips were removed and fixed by immersion in PB + 2% formaldehyde + 0.1% Triton X-100 for 10 min at 0°C, followed by methanol postfixation and

[2] The MT polymerizing buffer used in this work, PB, was incorrectly described in an earlier paper (20) due to a typographical error. The correct buffer contains 1 mM EGTA and no EDTA.

anti-tubulin immunofluorescence as usual. For electron microscopy, chromosomes were incubated with or without tubulin as above, and 10^6 were sedimented per coverslip. Formaldehyde fixation was as above, but the methanol step was omitted. Monoclonal anti-β tubulin incubation was performed as usual, followed by incubation with 5-nm gold goat anti-mouse IgG (Janssen Pharmaceutica, Beerse, Belgium) according to the manufacturers instructions (1:3 dilution for 90 min). After washing and postfixing with 1% glutaraldehyde in 0.1 M Na cacodylate pH 7.4 for 10 min at 25°C, the coverslips were osmicated, block stained, and processed as described, but without tannic acid treatment (13).

RESULTS

Isolation of Chromosomes with Functional Kinetochores

We have isolated an enriched fraction of metaphase chromosomes from CHO cells that retain functional properties. The method of mitotic arrest is important. Arrest with a high concentration of vinblastine results in a preparation of kinetochores essentially devoid of bound tubulin (see below). Exposure of the chromosomes to a buffer containing polyamines and EDTA strengthens them against mechanical stress (3). The final preparation is enriched for metaphase chromosomes and is essentially free of soluble cellular components, though variable amounts of cytoskeletal material and undisrupted spindles are present. The functional attributes of the kinetochore are labile after isolation, so we did not attempt further purification. The preparation was either used within 1 h of isolation, or frozen as aliquots in liquid nitrogen and stored at −80°C. Identical results were obtained with fresh or frozen chromosomes; most of the experiments were performed with the latter and confirmed using fresh material.

Microtubule Nucleation by Kinetochores: Kinetics

When chromosomes were incubated with phosphocellulose-purified tubulin, they nucleated MTs which could be clearly seen to emanate from the primary constriction of the chromatin, as defined by Hoechst counter staining (Fig. 1, *a* and *b*). The general appearance of this kinetochore nucleation was similar to that observed in previously published studies (2, 37, 38). The chromosome preparations were variably contaminated with mitotic centrosomes, which could be easily distinguished from the kinetochores in the nucleation assay (Fig. 1). Comparing the MTs grown off centrosomes and kinetochores, it was immediately apparent that the kinetochore MTs were more variable in length and generally shorter than were the centrosomal ones (compare parts *a* and *d* of Fig. 1). This phenomenon was investigated by assembling MTs from a mixture of chromosomes, thus contaminating mitotic centrosomes and axonemes, in a procedure analogous

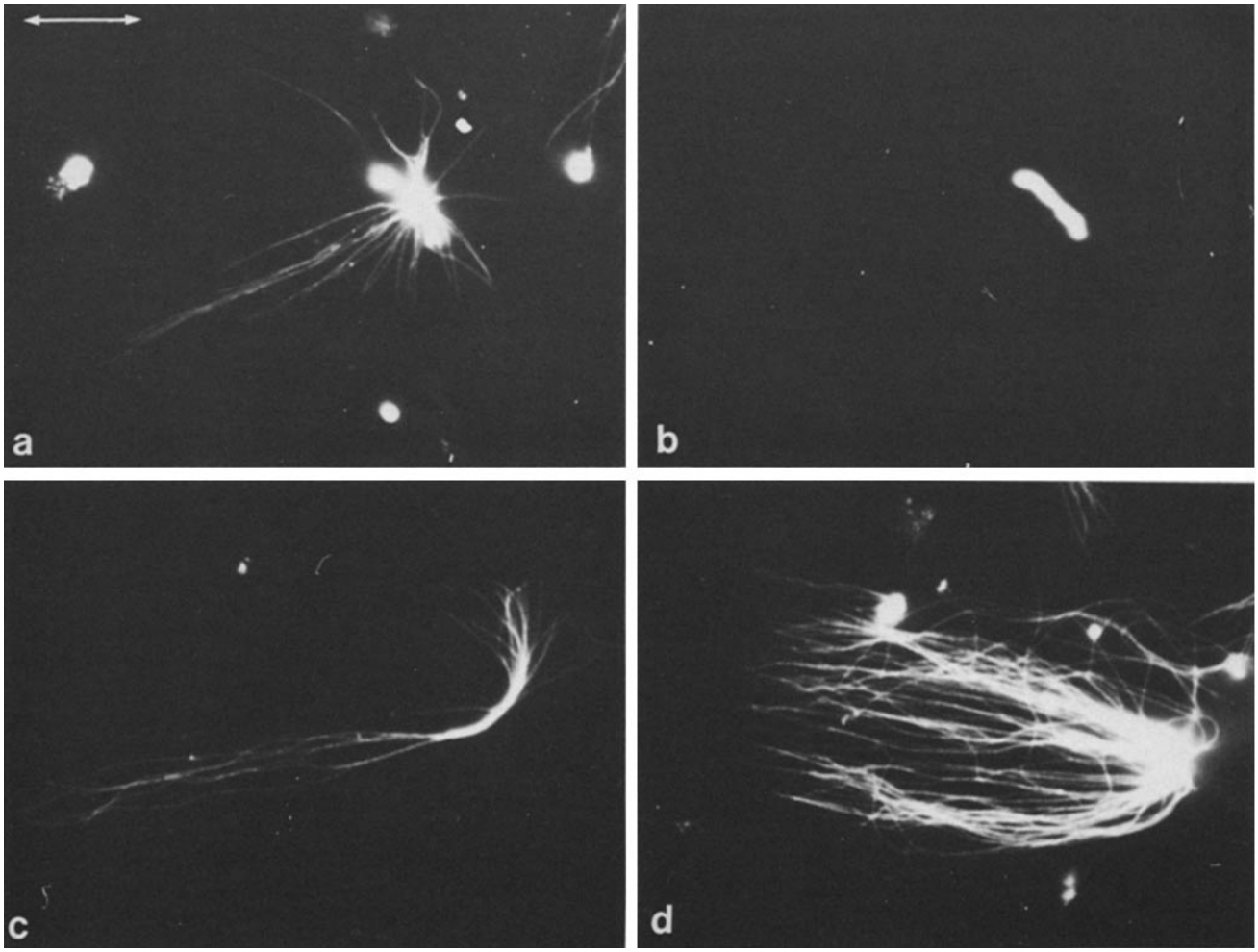

FIGURE 1 Microtubule nucleation by a mixture of chromosomes, mitotic centrosomes, and axonemes. These organelles were incubated together in 17 μM tubulin for 18 min at 37°C, fixed, sedimented onto coverslips, and visualized by anti-tubulin immunofluorescence (*a*, *c* and *d*) and Hoechst staining (*b*). All are taken from the same coverslip, and *a* and *b* are double exposures of the same field. Bar, 10 μm. (a and *b*) Kinetochore nucleation by chromosomes; (*c*) axoneme; (*d*) centrosome.

to that described by Bergen, Kuriyama, and Borisy (2). MT length distributions were measured at three time points, and the mean lengths as a function of time are shown in Fig. 2. As expected from previous studies, MTs nucleated by axonemes elongated at a constant rate. At the concentration of tubulin used, the plus ends (1.9 μm/min) grew faster than did the minus ends (0.7 μm/min) by a factor of ~2.7. The mean centrosomal MT length increased at the same rate as axoneme plus ends, in agreement with earlier studies (2). However, in contrast to previous studies (2, 37), the kinetochore MTs mean length increased at a much slower rate, similar to that of axoneme minus ends. The length distributions at 6 min are shown in Fig. 3. Inspection of length histograms revealed that while the centrosome and axoneme plus end length distributions were quite similar, those of the kinetochore and axoneme minus ends differed considerably. The kinetochore nucleated significant numbers of MTs longer than any from the axoneme minus end, and the peak of length distribution was broader in both directions. Similar results were obtained at later time points. It was thus not possible to draw conclusions about the polarity of the kinetochore MTs from length measurements alone.

Microtubule Nucleation by Kinetochores: Polarity

To get unambiguous data on the polarity of MT growth from the kinetochore, it was necessary to measure both the instantaneous rate of growth and the site of subunit addition. This would avoid complexities caused in the analyses of total MT length caused by asynchronous nucleation. Both of these goals could be achieved by the use of a functional labeled tubulin molecule that could be distinguished from unlabeled tubulin in the immunofluorescence assay. We chose biotin labeling because the small, hydrophilic biotin moiety seemed likely to cause minimal perturbation of tubulin function. MTs

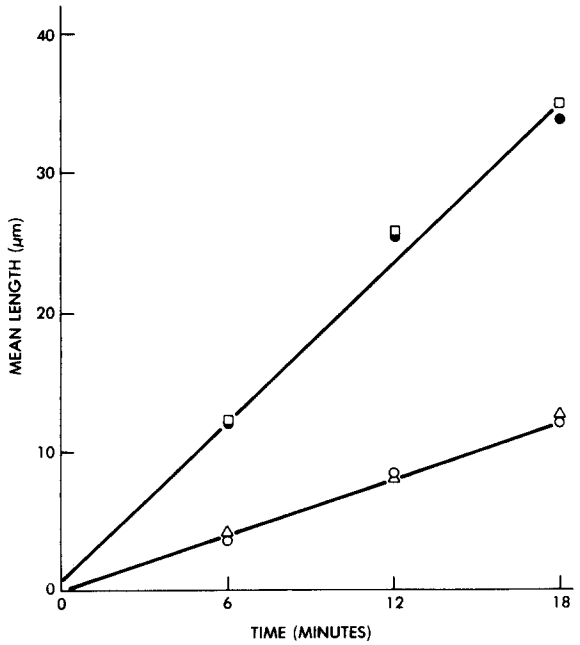

FIGURE 2 Mean length of MTs nucleated by the organelles shown in Fig. 1. At least 100 MTs were measured for each time point. These conditions are the same as those in Fig. 1. ●, axoneme plus ends; ○, axoneme minus ends; △, kinetochores; □, centrosomes. The lines are best fits by linear regression through the axoneme points, including the origin.

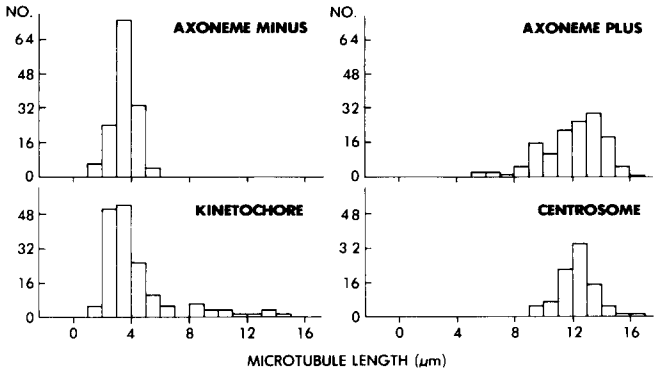

FIGURE 3 Length histograms for the 6-min time point in Fig. 2.

were reacted with *N*-hydroxysuccinimidyl biotin, and then active biotinylated subunits were selected by a subsequent round of assembly. Providing the stoichiometry of labeling was kept below four biotins per dimer, the yield from such a protocol was excellent (20–50% of starting tubulin was recovered as active dimer), and normal MTs were formed. The modified tubulin was inhibited in its rate of polymerization onto an axoneme template compared with unmodified tubulin, to an extent which increased with the stoichiometry of labeling. The tubulin used in Figs. 4 and 5 had a stoichiometry of ~four to five biotins per dimer, which significantly retarded assembly (see below).

To measure the instantaneous rate of subunit addition axonemes (Fig. 4, *a* and *b*), chromosomes (Fig.4, *c* and *d*), and CHO interphase centrosomes (Fig. 4, *e* and *f*) were incubated first with unmodified tubulin and allowed to nucleate MTs. Biotinylated tubulin was then added, and after a sufficient time for the addition of a biotinylated segment onto the unlabeled MTs, the mixture was fixed and visualized as described in Materials and Methods. Labeled segment lengths typical of plus and minus end lengths can readily be distinguished, particularly off the axoneme template. The labeled segments were measured, and length distributions for axoneme plus and minus ends, and centrosomes (Fig. 5, *a* and *b*) or axonemes and kinetochores (Fig. 5, *c* and *d*) are shown. As can be seen from Fig. 5, *a* and *b*, the length distribution of labeled segments from centrosomes is consistent with >95% plus ends distal to the centrosome, confirming the result of Bergen, Kuriyama, and Borisy (2). Thus, the fidelity of polarity specification by centrosomes nucleating in vitro is comparable to that found in vivo (13). A few completely labeled MTs were also observed emanating from the centrosome, with the same length as the added labeled segments (Fig. 4, *e* and *f*). These probably represent MT renucleation after the addition of labeled tubulin. The results with kinetochores (Fig. 5, *b* and *c*) were quite different, consistent with approximately equal numbers of plus and minus ends growing distal to the organizing center (Fig. 5, *c* and *d*). The frequency of MTs with each polarity cannot be accurately determined because the high density of MTs close to the kinetochore tends to obscure detail there (Fig. 4, *c* and *d*), so minus ends may be under-represented. Many MTs emanating from kinetochores were fully labeled; these were presumably nucleated after the pulse of biotinylated tubulin. The fact that there are more fully labeled MTs associated with the kinetochores than with the centrosomes probably results from the apparent ability of kinetochores to nucleate assembly continuously (see Fig. 10). This also contributes to the broad length

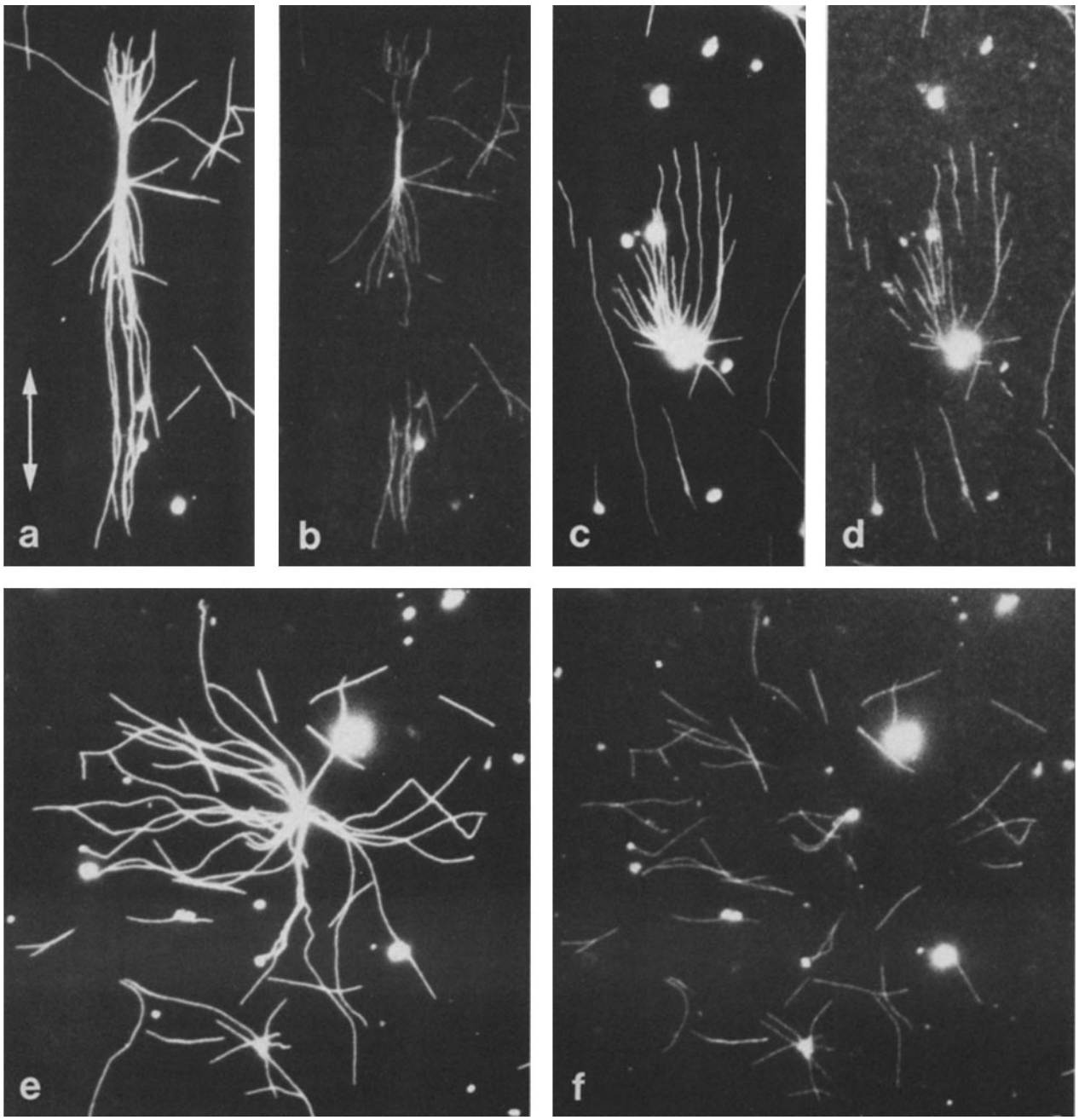

FIGURE 4 Polarity assessment using biotinylated tubulin. A mixture of chromosomes and axonemes or interphase centrosomes and axonemes was incubated first with unlabeled tubulin to allow nucleation, and then biotin-labeled tubulin was added (see Materials and Methods). *a*, *c* and *e* show total MTs, visualized with mouse anti-tubulin and fluorescein isothiocynate goat anti-mouse IgG. *b*, *d*, and *f* shown biotin-labeled segments only, visualized with Texas Red-labeled strepavidin. Bar, 12 μm. (a and *b*) Axoneme. (*c* and *d*) Chromosome. Hoechst counterstain is not shown, but the MTs arise from the primary constriction region. Note the presence of labeled segments of both plus and minus end lengths. (*e* and *f*) Centrosome. Note fully biotinylated MTs arising directly from the centrosome. All labeled segments are of plus end length.

distribution seen in Fig. 3. No evidence of proximal subunit addition was seen with any of the organelles in these experiments, or when the order of addition of unmodified and modified tubulin was reversed.

The growth rate of the MTs after addition of biotinylated tubulin can be compared with that for unlabeled tubulin. The plus ends in Fig. 5, *a* and *b*, grew ~0.84 μm/min, and in Fig. 5, *b* and *c*, 1.0 μm/min at a total tubulin concentration of ~32 μM. Unmodified tubulin at the same concentration grows at ~4 μm/min (21), indicating that the biotinylated tubulin is considerably inhibited in its addition rate under these stringent in vitro conditions, without glycerol or MAPs. However, the ratio of plus to minus end growth rates was similar to that of unmodified tubulin, so the conclusions from Fig. 5 are not prejudiced by the diminished assembly rate. All MTs had distal-labeled segments and could be assigned as plus or minus end distal with a high degree of certainty on the basis of growth rates. Kinetochores thus appear to nucleate MTs of mixed polarity under these conditions. In more recent experiments, we have used less heavily modified tubulin (two

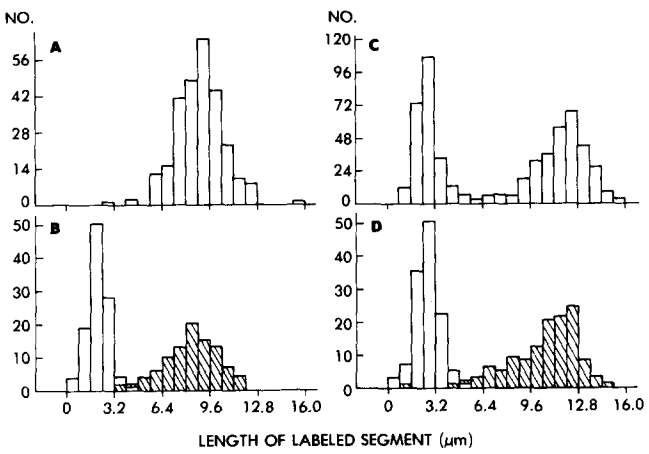

FIGURE 5 Length distribution of biotin-labeled segments for the experiments shown in Fig. 4. (*a* and *b*) Experiment using interphase centrosomes and axonemes. (*a*) Centrosomes. (*b*) Axonemes. ▩, plus ends; □, minus ends. (*c* and *d*) Experiment using chromosomes and axonemes. (*c*) Kinetochores. Note bimodal length distribution. (*d*) Axonemes. ▩, plus ends; □, minus ends.

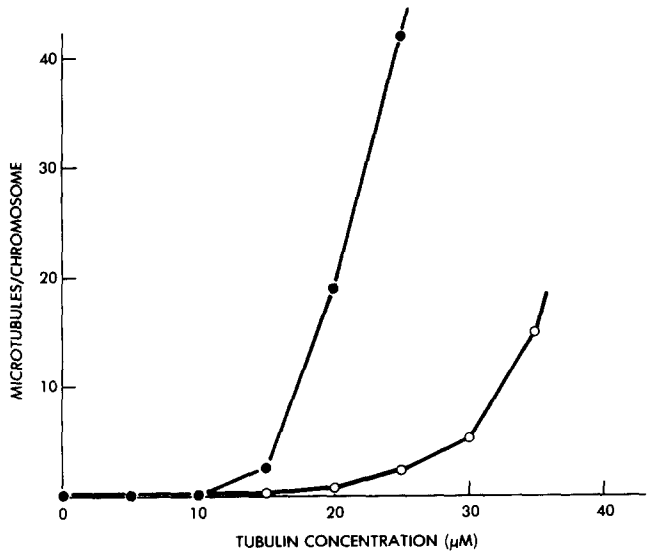

FIGURE 6 Kinetochore nucleation as a function of tubulin concentration. 100 chromosomes were counted and averaged for each point. ○, 5-min incubation; ●, 15-min incubation.

biotins per dimer or less). These preparations are much less inhibited in their assembly properties. Further improvements in visualization technology (23) may allow us to go to even lower stoichiometries.

Microtubule Nucleation by Kinetochores: Concentration Dependence

To assess the capacity of the kinetochore as a nucleating agent compared with centrosomes or MT fragments, we studied the dependence of the number of MTs nucleated by kinetochores on tubulin concentration. As shown in Fig. 6, MTs were first seen at 15 μM tubulin, and the number per kinetochore rose steeply with concentration. Concentrations higher than 35 μM gave further increases in number, but these became difficult to count accurately. The steady state concentration for this tubulin preparation is 14 μM (20), though it may have been reduced by the conditions of the chromosome assay to ~10 μM (reference 23; Fig. 1). Thus, kinetochores, unlike centrosomes (20, 21), do not appear to nucleate below the steady state concentration for free MTs within a 15-min incubation period. We could observe kinetochore nucleation because even above the steady state concentration, the spontaneous assembly of MTs (with purified tubulin in aqueous buffer), though thermodynamically feasible, is kinetically unfavorable (26). In the paper that follows (23), we examine the possibility that the observed nucleation was the result of an association of spontaneously assembled MTs with the kinetochore, and conclude that this is probably not a significant factor under these conditions. It was clear that the kinetochore in vitro could nucleate many more MTs than are found in the kinetochore fiber in vivo at metaphase (9–16 for CHO cells [40]). The data at 5 and 15 min indicated that the number of MTs is not constant with time, whereas it is for centrosomes (16). This was further investigated in more detail below.

Microtubule Nucleation by Kinetochores: Electron Microscopy

Representative kinetochores after nucleating MTs are seen in thin section in Fig. 7. The dense outer plate of the kinetochore is clearly seen, although it is somewhat thicker and more diffuse than that seen for kinetochores fixed in vivo, perhaps as a result of drug treatment and/or isolation procedures. The clear zone is easily seen, as is the "fibrous corona" material (see also Fig. 9), though the inner dense plate is not clearly visualized. The kinetochore-nucleated MTs appear in various orientations. Some clearly run tangential to the kinetochore plate (seen in cross-section in Fig. 7*b*), interacting laterally with the plate or the fibrous corona. Others are perpendicular to the plate, often penetrating it, and can usually be seen traversing the clear zone and penetrating into the chromatin (arrow in Fig. 7*a*). MTs were seldom observed terminating at the plate, but MT ends are difficult to localize in random thin sections. These observations are consistent with the MTs being nucleated in the fibrous corona with random orientation, as has been suggested earlier (32), and then elongating on both ends.

Tubulin Binding by Kinetochores

We noticed that kinetochores were brightly stained by anti-tubulin after nucleation assays. This phenomenon was further investigated by observing chromosomes incubated with tubulin under conditions where MTs were not nucleated. Chromosomes incubated in the presence of tubulin at 37°C acquired material reacting with anti-tubulin antibody, localized to a bright pair of dots at the primary constriction (Fig. 8, *a* and *b*). These co-localized at the light level with centrosome determinants recognized by serum from a patient suffering from CREST scleroderma (4) in double-staining studies (data not shown). Control chromosomes incubated without tubulin showed no staining (Fig. 8, *c* and *d*), as did untreated chromosomes. Although some chromosomes showed occasional dots of staining not at the kinetochore, the kinetochore dots were the only region stained on all chromosomes. The brightness of the dots, however, showed considerable variability between chromosomes. The lack of quantitative assay has so far prevented detailed study of the interaction between the kinetochore and soluble tubulin. The intensity of anti-tubulin

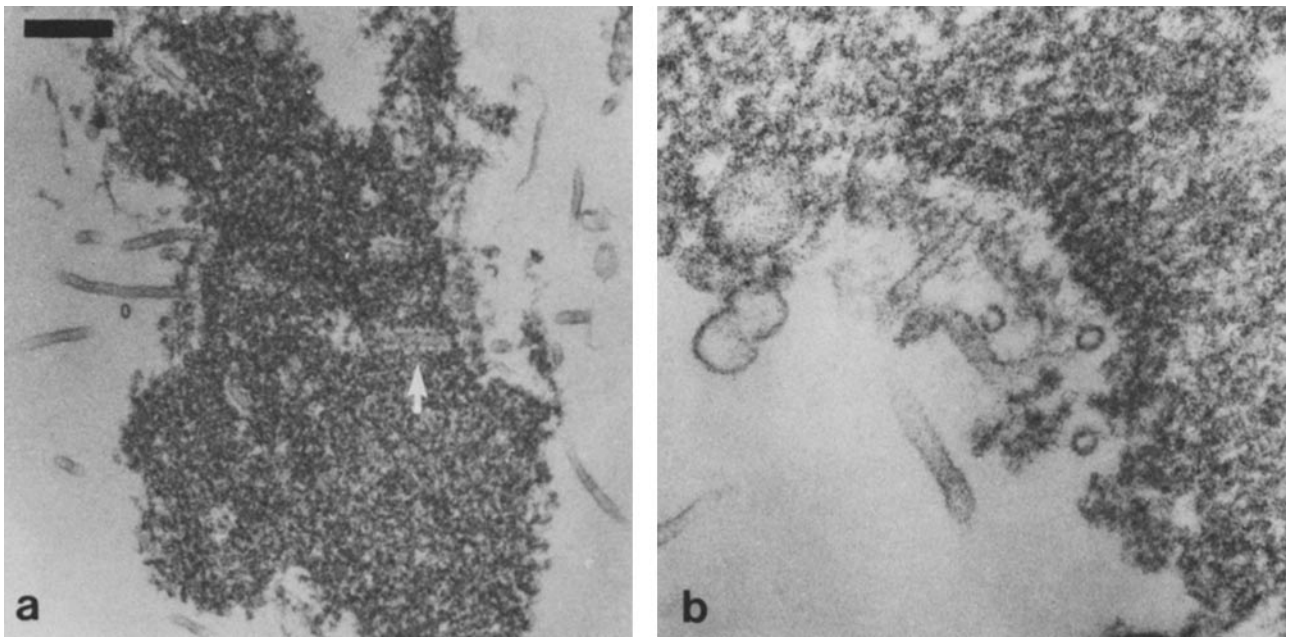

FIGURE 7 Electron microscopy of kinetochores after MT nucleation. Note the presence of MTs penetrating the kinetochore and chromatin (arrow in *a*) and of MTs running tangential to the kinetochore, seen as cross-sections in *b*. The appearance of kinetochores before nucleation was as in Fig. 9. Bar, 2 μm in *a*; 0.9 μm in *b*.

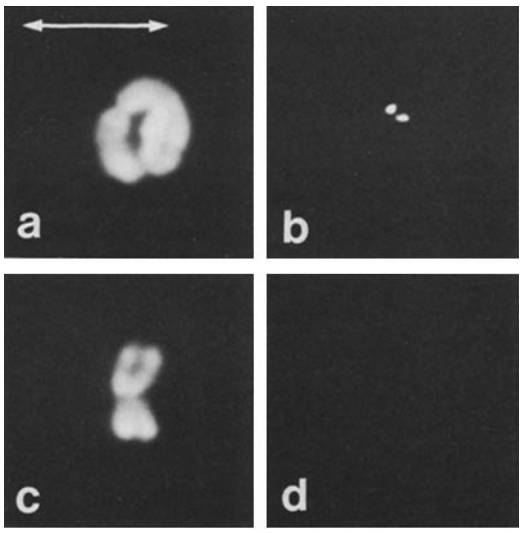

FIGURE 8 Tubulin binding by kinetochores. Chromosomes were incubated for 10 min at 37°C either in the presence (*a* and *b*) or absence (*c* and *d*) of 10 μM tubulin. They were then diluted into cold buffer and sedimented unfixed onto coverslips. The coverslips were fixed with formaldehyde and then methanol, and visualized by anti-tubulin immunofluorescence (*a* and *c*) and Hoechst counter staining (*b* and *d*). Untreated chromosomes appeared identical to *c* and *d*. Bar, 8 μm. (*a* and *b*) The same field after incubation with tubulin; (*c* and *d*) the same field after incubation without tubulin.

TABLE I. *Tubulin Binding by Kinetochores In Vitro*

Incubation condition	Anti-tubulin staining at kinetochore
None	–
PB, 37°C, 10 min	–
PB, 10 μM tubulin, 0°C, 10 min	–
PB, 10 μM tubulin, 37°C, 3 min	+
PB, 10 μM tubulin, 37°C, 10 min (Std)	++
Std + 20 mg/ml BSA	++
Std + 5 mM $CaCl_2$	++
Std, preincubate 100 μM colcemid	++
Std, preincubate 50 μM nocodazole	++

Chromosomes were incubated as described, then sedimented through a glycerol cushion onto coverslips. After formaldehyde and methanol fixation, bound tubulin was visualized by immunofluorescence with anti-tubulin.

immunofluorescent staining was estimated by eye, and the results for various treatments are shown in Table I. The binding reaction appeared to be time and temperature dependent, occurred poorly, if at all, at 0°C and was not inhibited by an excess of BSA. The binding appeared to be very tight, since it was not reversed by sedimentation through the glycerol cushion or by incubation at 37°C after extensive dilution. The physical form of bound tubulin is not known, but it is very unlikely to be in the form of short MTs for a number of reasons: (a) None were seen at the electron microscopic level (Fig. 9). (*b*) Preincubation of tubulin with colcemide or nocodazole for 10 min (Table I) had no effect on binding, nor did addition of $CaCl_2$ to 5 mM, though all these additions completely abolished MT nucleation at a higher tubulin concentration. (*c*) GDP tubulin and *N*-ethyl maleimide–treated tubulin were also able to bind, though neither can polymerize into MTs under these conditions (data not shown). (*d*) Incubation of kinetochores with tubulin below 15 μM resulted in no MT growth (Fig. 6), but gave strong kinetochore staining (Fig. 8). Extensive MT growth would have been expected off MT seeds at these concentrations if they were present (21).

To better understand the role of bound tubulin in the kinetochore, an attempt was made to localize it at the ultrastructural level using immunogold labeling. Kinetochores were incubated with or without tubulin, sedimented onto coverslips, and stained with monoclonal anti-tubulin, then with affinity purified goat anti-mouse IgG adsorbed to 5-nm gold particles. The results are shown in Fig. 9. In the kinetochores incubated with tubulin, gold particles were observed

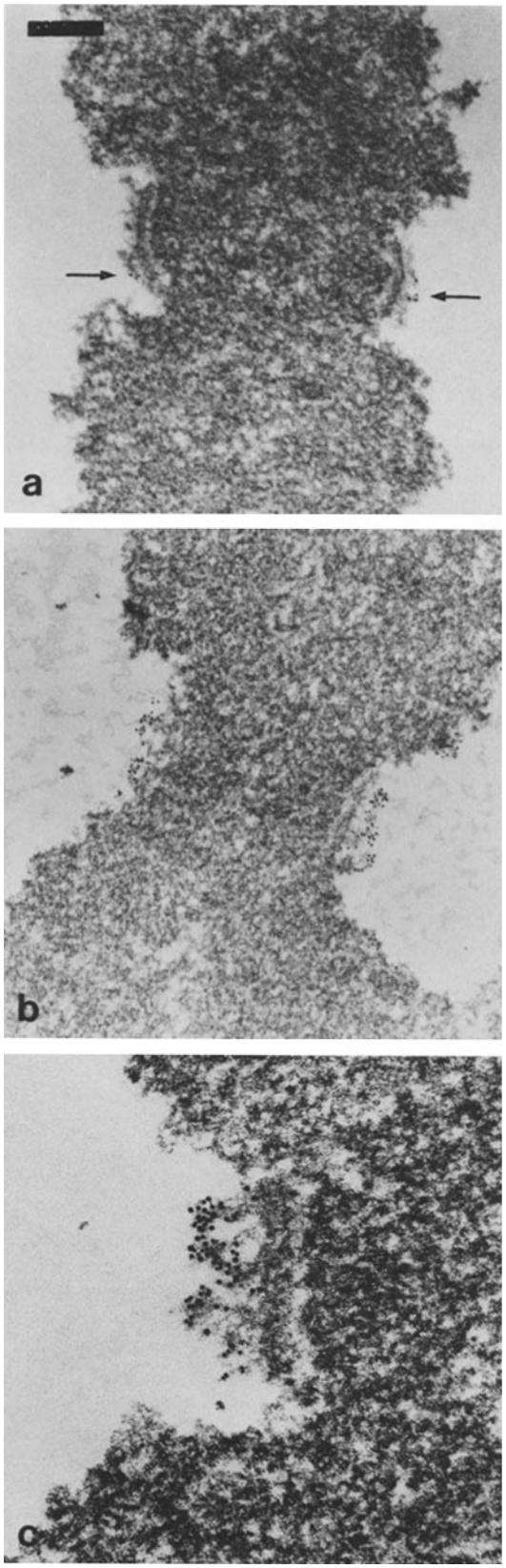

FIGURE 9 Tubulin binding at the electron microscopic level. Visualization by 5-nm colloidal gold binding. Incubations are the same as for Fig. 8, and immunogold staining is as in Materials and Methods. (*a*) Control incubated without tubulin. Some gold is bound to the kinetochore region (arrows). The fibrous corona is well visualized. (*b* and *c*) Incubated with 10 μM tubulin. Note the heavy gold binding to the corona region in front of the kinetochore plate. Bar, 2.5 μm in *a* and *b*; 0.8 μm in *c*.

in the region of the corona, bound to poorly defined fibrous or amorphous material that appeared to emanate from the outer plate. Very little binding to either the outer plate itself or more internal regions of the kinetochore was seen (Fig. 9, *b* and *c*). In contrast, published results using CREST sera show mainly staining of internal regions of the kinetochore (4). The number of gold particles on the kinetochore was counted for many random 50-nm sections. For kinetochores incubated with tubulin, the average number of gold particles per section was $m = 67$ (SD = 33, $n = 94$). For control kinetochores with no tubulin incubation $m = 8$ (SD = 6.5, $n = 88$), and for equivalent nonkinetochore regions of the chromosome, less than one gold particle was bound with or without tubulin incubation. Thus, incubation with tubulin in vitro leads to a highly significant increase in the amount bound to the fibrous corona.

Role of Bound Tubulin

We were interested in whether tubulin bound to the fibrous corona has an effect on kinetochore function, and in particular whether it is involved in MT nucleation. This could be tested in two ways: (*a*) by comparing the properties of kinetochores with and without tubulin preincubations in vitro, and (*b*) by comparing kinetochores isolated from vinblastine- and colcemid-arrested cells. The results of an in vitro preincubation experiment are shown in Fig. 10. Chromosomes were preincubated in 30 μM tubulin for 15 min at 37°C, during which time extensive tubulin binding and MT nucleation occurred. They were then cooled to 0°C for 10 min, causing complete depolymerization of existing MTs but no reversal of tubulin binding. The lack of remaining MT fragments was demonstrated in a control experiment in which the preincubated, cooled chromosomes were challenged with

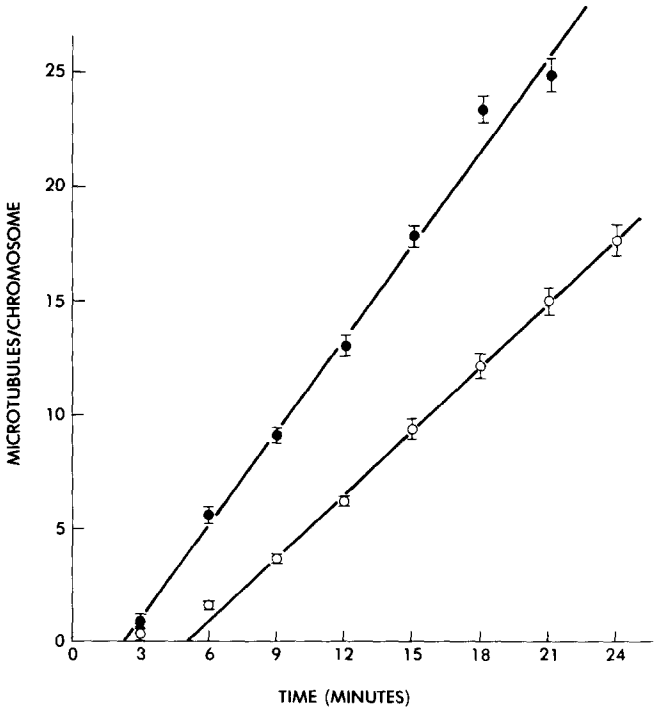

FIGURE 10 Number of MTs nucleated per chromosome as a function of time. 100 chromosomes were averaged per time point. ○, no preincubation; ●, chromosomes preincubated in 30 μM tubulin for 15 min at 37°C, followed by 10 min at 0°C. The final tubulin concentration was 15 μM in both cases.

tubulin at 10 μM, which allows extensive growth off MT fragments or axonemes (21), but none off kinetochores (Fig. 6). No nucleation was seen, which indicates the absence of residual cold stable MT fragments (data not shown). The preincubated, cooled chromosomes were compared with untreated controls for their nucleation capacity at 15 μM tubulin, taking care to allow for the tubulin present in the preincubation mix. (This fraction [25%] of the tubulin in the control was provided by control tubulin also preincubated at 37°C for 15 min). Fig. 10 shows the number of MTs nucleated per chromosome as a function of time for chromosomes with and without preincubation. The control chromosomes showed a distinct lag phase, after which the number of MTs nucleated increased linearly with time. The phenomena of continuous nucleation and growth must have contributed to the broad distribution MT lengths for MT nucleated by kinetochores (Fig. 3). The kinetochores with tubulin already bound show a decreased lag and an increased slope relative to the controls. Indeed the true lag may be reduced almost to zero after tubulin preincubation, since MTs must be of significant length before they can be counted in the light microscope. We estimate this minimum length to be 1–2 μm, and as MT plus ends grow at ~1.8 μm/min at 15 μm tubulin, the observed 2-min lag phase may mean that some MTs in the preincubated sample (but not the control) were initiated immediately upon introducing the chromosomes into a solution of prewarmed tubulin. A different control for this experiment would have been to preincubate chromosomes in PB and GTP in the absence of tubulin. We found, however, that such treatment caused a variable but extensive inhibition of kinetochore nucleation capacity. This was not prevented by including protease inhibitors in the preincubation buffer, but could be offset to some extent by increasing the magnesium concentration in the preincubation, or by omitting the GTP. Since preincubation of kinetochores usually results in extensive loss of activity, the increased nucleation capacity seen in Fig. 10 indicates that bound tubulin actually protects the kinetochore against inactivation, as well as enhancing nucleation capacity.

Effect of the Drug Used for Mitotic Arrest on the Properties of Isolated Chromosomes

It was of interest to compare the nucleation properties of vinblastine kinetochores with those prepared from cells arrested with colcemid. We found that colcemid kinetochores nucleated many more MTs than did vinblastine kinetochores at all tubulin concentrations tested (compare parts *a* and *b* of Fig. 11), and that the threshhold concentration for the onset of polymerization was lower, comparable to that of centrosomes. Comparing colcemid kinetochores with centrosomes, it was clear that the colcemid kinetochores nucleated large numbers of plus end out MTs with no lag phase. Shorter MTs were also present, but they tended to be obscured (Fig. 11 *b*). Problems visualizing short MTs near the chromosome may have contributed to minus end out MTs being missed in earlier studies (2, 35). Untreated colcemid kinetochores were brightly stained by anti-tubulin (Fig. 11, *c* and *d*), in contrast to vinblastine kinetochores (Fig. 8). Thus, tubulin binding correlates with enhanced nucleation capacity, as with preincubation in vitro. No differences were detected by electron

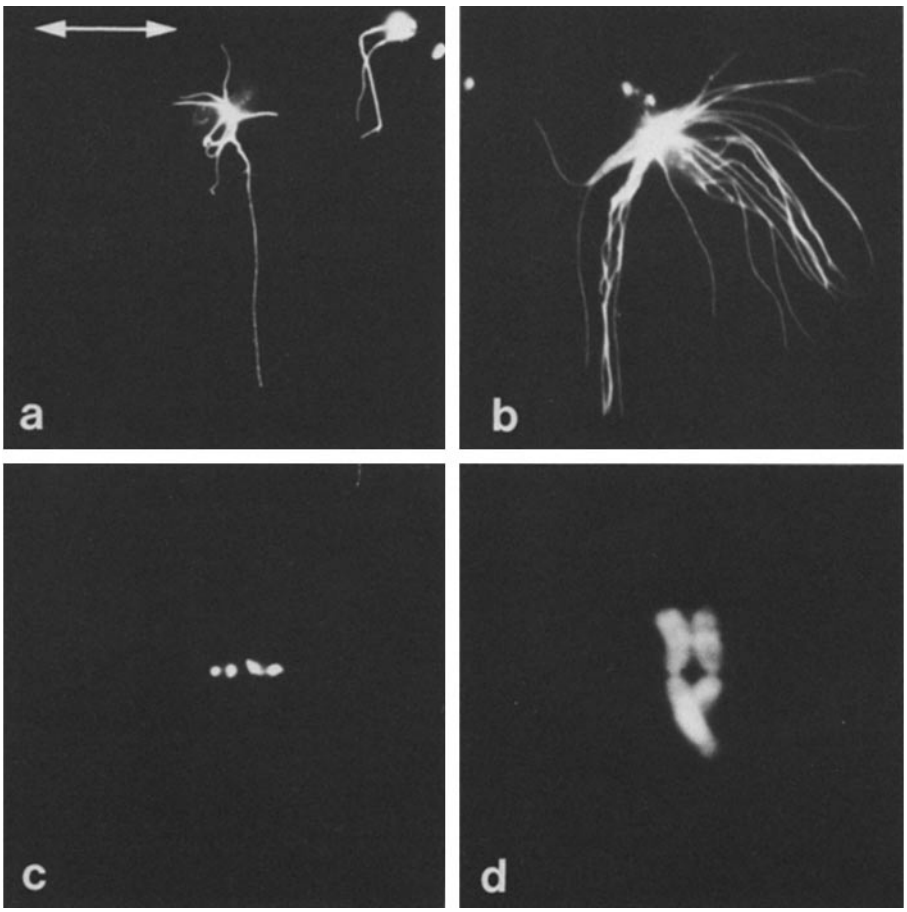

FIGURE 11 Visual comparison of the properties of vinblastine chromosomes and colcemid chromosomes. Chromosomes were isolated from cells arrested for 5 h in the presence of 10 μg/ml vinblastine (*a*) or 0.1 μg/ml colcemid (*b*, *c*, and *d*). Microtubule nucleation at 10 min in 15 μM tubulin is shown in *a* for a vinblastine chromosome and *b*, a colcemid chromosome. Note the large number of long MTs in *b*. *c* and *d* show a double exposure of untreated colcemid chromosomes stained with anti-tubulin (*c*) and Hoechst (*d*) prepared as for the tubulin binding assay. Note the strong staining of the kinetochore region. The vinblastine chromosomes appeared as shown in Fig. 8, *c* and *d*, with no tubulin staining. Bar, 14 μm in *a* and *b*; 8.5 μm in *c* and *d*.

microscopy between vinblastine and colcemid chromosomes (data not shown).

DISCUSSION

Studies of the kinetochore in vitro have two distinct but related goals: (*a*) to understand the functional properties of the organelle, and relate these to the dynamics and morphogenesis of the mitotic spindle in vivo, and (*b*) to try to approach the chemistry underlying these functional properties. The observation in this paper most important to kinetochore chemistry may be the demonstration of tubulin binding by the corona material. This part of the kinetochore has frequently been described (15, 30, 32), and Pickett-Heaps in particular has emphasized its potential importance on structural grounds (28, 34). The observation of an essentially irreversible tubulin binding site on this structure may facilitate its isolation and molecular characterization. The assay for this binding site depended on chromosomes being isolated without bound tubulin, and this varied with the drug used for mitotic arrest. Vinblastine gave kinetochores with very little tubulin detectable by immunofluorescence (Fig. 8, *b* and *c*), whereas colcemid gave kinetochores with bright staining (Fig. 11, *b* and *c*). This difference could arise because vinblastine treatment results in cellular tubulin becoming sequestered into paracrystals (1), whereas the colcemid–tubulin complex is soluble and could bind to the kinetochore in vivo as it does in vitro. Alternatively, the difference could arise from the more potent MT depolymerizing conditions induced by vinblastine. The physical form of bound tubulin is unknown. No MT stubs were seen in the electron microscope after tubulin incubation in vitro or on colcemid chromosomes, and binding was not inhibited by drugs or calcium (Table I), which prevent MT polymerization. However, the binding was time and temperature dependent, suggesting a mechanism more complex than simple electrostatic interaction, for example. Bound tubulin may be a normal structural component of metaphase kinetochores (25). Alternatively, if the primary role of the corona is something other than nucleation, tubulin binding may label a site normally used as part of some more complex reaction with MTs.

The possible relationship between tubulin binding and MT nucleation is particularly interesting: The correlation of bound tubulin with enhanced nucleation capacity (Figs. 10 and 11) suggests that nucleation at the kinetochore may involve an interaction between organelle bound and soluble tubulin. A role for bound tubulin in site-specific MT nucleation was previously proposed by Pepper and Brinkley (26) on the basis of inhibition by tubulin antibody. However, we have seen no effect of preincubation with monoclonal antibodies to tubulin on MT nucleation. The observed concentration dependence of nucleation with vinblastine chromosomes (Fig. 6) may result from the interaction of two concentration-dependent processes—tubulin binding to nontubulin sites on the kinetochore and tubulin–tubulin interactions involving both free and bound tubulin. These two processes may also give rise to the complex kinetics of nucleation (Figs. 2, 3, 5, and 10). Since the tubulin binding sites are mainly in the corona material, most of the nucleation may also occur here, and this possibility is supported by the electron microscopy of nucleated MTs in this and earlier studies (32).

Nucleation at the kinetochore in vivo has been carefully characterized at the ultrastructural level by following cells released from a drug block (10). These studies indicate that the first observable stage in nucleation is the formation of small, randomly oriented MTs in the vicinity of the kinetochore plate. The in vitro studies suggest that this localized but apparently disordered assembly may be due to the presence of a high concentration of tubulin in the vicinity of the kinetochore, as a result of binding to corona material. Such bound tubulin could explain the postulated local region of lowered critical concentration near the kinetochore in vivo (9).

An important question concerns the contribution of kinetochore nucleation to the formation of the kinetochore fiber in vivo. Although the kinetochore can nucleate both in vivo (10, 39) and in vitro (2, 18, 26, 36–38), the question of whether it does so during a normal mitosis is unresolved (28, 30, 35). We feel that caution should be exercised in interpreting the results of experiments where cells are released from drug blocks, since the unphysiologically high tubulin concentration after release may force nucleation. In addition, the bound drug–tubulin complex could play a role in nucleation. The properties of the nucleation process described here make it difficult to see how the MTs nucleated by the kinetochore can become incorporated into an ordered kinetochore fiber. In particular, the observation of mixed polarity of nucleation (Figs. 4 and 5) is difficult to reconcile with the homopolar kinetochore fiber. The concentration dependence of nucleation (Fig. 6) and the lag phase (Fig. 10) show that the kinetochore, at least as isolated from vinblastine-arrested cells and without prior tubulin exposure, is inefficient at nucleating compared with the centrosome. The latter is clearly an efficient nucleating element, which can nucleate well below the steady state concentration (20) with a specific polarity (Figs. 4 and 5) (2). If the dynamics of MT assembly ensure that the free tubulin concentration in a mitotic cell is at or below the steady state concentration, then the kinetochore may only be able to nucleate poorly, if at all during a normal prometaphase (for a fuller discussion, see reference 22). Thus, we support the older idea that the kinetochore fiber is formed by the interaction of the kinetochore with MTs emanating from the poles. Experimental support for this idea is discussed in the paper that follows (23).

We thank S. Blose for the generous gift of anti-tubulin, F. McKeon for CREST human anti-kinetochore serum, L. Evans for help with electron microscopy, and C. Cunningham-Hernandez for help in preparing the manuscript. We gratefully acknowledge useful discussions with U. Euteneuer, J. R. McIntosh, W. Earnshaw, and F. McKeon as well as corrections to the manuscript by J. R. McIntosh and T. Pollard.

This work was supported by grants from the American Cancer Society and the National Institutes of Health.

Received for publication 6 March 1985, and in revised form 1 April 1985.

REFERENCES

1. Battacharyya, B., and J. Wolf. 1976. Tubulin aggregation and disaggregation. Mediation by two distinct vinblastine binding sites. *Proc. Natl. Acad. Sci. USA.* 73:2375–2378.
2. Bergen, L. G., R. Kuriyama, and G. G. Borisy. 1980. Polarity of microtubules nucleated by centrosomes and chromosomes of Chinese hamster ovary cells in vitro. *J. Cell Biol.* 84:151–159.
3. Blumenthal, A. B., J. D. Dieden, L. N. Kapp, and J. W. Sedat. 1979. Rapid isolation of metaphase chromosomes containing high molecular weight DNA. *J. Cell Biol.* 81:255–259.
4. Brenner, S. L., and B. R. Brinkley. 1982. Tubulin assembly sites and the organization of microtubule arrays in mammalian cells. *Cold Spring Harbor Symp. Quant. Biol.*

46:241–254.
5. Brent-Heath, I. 1980. Variant mitoses in lower eukaryotes: indicators of the evolution of mitosis. *Int. Rev. Cytol.* 64:1–80.
6. Brent-Heath, I. 1981. Mitosis through the electron microscope. *In* Mitosis/Cytokinesis. A. M. Zimmerman and A. Forer, editors. Academic Press, Inc., New York. 245–275.
7. DeBrabander, M. 1982. A model for the microtubule organizing activity of the centrosomes and kinetochores in mammalian cells. *Cell Biol. Int. Rep.* 6:901–915.
8. DeBrander, M., G. Geuens, J. DeMey, and M. Joniau. 1981. Nucleated assembly of mitotic microtubules in living PtK_2 cells after release from nocodazole block. *Cell Motil.* 1:469–483.
9. Ellis, G. W., and D. A. Begg. 1981. Chromosome micromanipulation studies in mitosis/cytokinesis. A. M. Zimmerman and A. Forer, editors. Academic Press, Inc., New York. 155–179.
10. Euteneuer, U., and J. R. McIntosh. 1981. Structural polarity of kinetochore microtubules in PtK_1 cells. *J. Cell Biol.* 89:338–345.
11. Evans, L., T. Mitchison, and M. Kirschner. 1985. Influence of the centrosome on the structure of nucleated microtubules. *J. Cell Biol.* 100:1185–1191.
12. Haimo, L. T., B. R. Telzer, and J. L. Rosenbaum. Dynein binds to and cross-bridges cytoplasmic microtubules. *Proc. Natl. Acad. Sci. USA.* 76:5759.
13. Heidemann, S. R., and J. R. McIntosh. 1979. Visualization of the structural polarity of microtubules. *Nature (Lond.).* 286:517–519.
14. Henderson, R., J. S. Jubb, and S. Whytock. 1978. Specific labelling of the protein and lipid on the extracellular surface of purple membrane. *J. Mol. Biol.* 123:259–274.
15. Jokelainen, P. T. 1967. The ultrastructure and spatial organization of the metaphase kinetochore in mitotic rat cells. *J. Ultrastruct. Res.* 19:19–44.
16. Kuriyama, R. 1984. Activity and stability of centrosomes of CHO cell in the nucleation of microtubules in vitro. *J. Cell Sci.* 66:277–295.
17. Lewis, C. D., and U. K. Laemmli. 1982. Higher order metaphase chromosome structure—evidence for metalloprotein interactions. *Cell.* 29:171–181.
18. McGill, M., and B. R. Brinkley. 1975. Human chromosomes and centrioles as nucleating sites for the in vitro assembly of microtubules from bovine brain tubulin. *J. Cell Biol.* 67:189–199.
19. McNeill, P. A., and M. W. Berns. 1981. Chromosome behavior after laser microirradation of a single kinetochore in mitotic PtK_2 cells. *J. Cell Biol.* 88:543–553.
20. Mitchison, T. J., and M. W. Kirschner. 1984. Microtubule assembly nucleated by isolated centrosomes. *Nature (Lond.).* 312:232–236.
21. Mitchison, T. J., and M. W. Kirschner. 1984. Dynamic instability of microtubule growth. *Nature (Lond.).* 312:237–241.
22. Mitchison, T. J., and M. W. Kirschner. 1984. Microtubules dynamics and cellular morphogenesis. *In* The Cytoskeleton. D. Murphy, D. W. Cleveland, and G. G. Borisy, editors. Cold Spring Harbor Laboratory, Cold Spring Harbor, NY.
23. Mitchison, T. J., and M. W. Kirschner. 1985. Properties of the kinetochore in vitro. II. Microtubule capture and ATP dependent translocation. *J. Cell Biol.* 101:766–777.
24. Nicklas, R. B., and C. A. Staehly. 1967. Chromosome micromanipulation. I. The mechanism of chromosome attachment to the spindle. *Chromosoma.* 21:1–16.
25. Pepper, D. A., and B. R. Brinkley. 1977. Localization of tubulin in the mitotic apparatus by immunofluorescence and immunoelectron microscopy. *Chromosoma (Berl.).* 60:223–235.
26. Pepper, D. A., and B. R. Brinkley. 1979. Microtubule initiation at kinetochores and centrosomes in lysed mitotic cells. Inhibition of site-specific nucleation by tubulin antibody. *J. Cell Biol.* 82:585–591.
27. Peterson, J. B., and H. Ris. 1976. Electron microscopic study of the spindle and chromosome movement in the yeast *Saccharomyces cerevisiae*. *J. Cell Sci.* 22:219–242.
28. Pickett-Heaps, J. D., D. H. Tippit, and K. R. Porter. 1982. Rethinking mitosis. *Cell.* 29:729–744.
29. Rieder, C. L. 1981. The structure of the cold stable kinetochore fibre in metaphase PtK_1 cells. *Chromosoma.* 84:145–158.
30. Rieder, C. L. 1982. The formation, structure and composition of the mammalian kinetochore and kinetochore fiber. *Int. Rev. Cytol.* 79:1–57.
31. Reider, C. L., and G. G. Borisy. 1981. Attachment of kinetochores to the prometaphase spindle in PtK_1 cells. *Chromosoma.* 82:693–716.
32. Ris, H., and P. L. Witt. 1981. Structure of mammalian kinetochore. *Chromosoma (Berl.).* 82:153–170.
33. Roos, U.-P. 1975. Mitosis in the cellular slime mode *Polysphondylium violaceum*. *J. Cell Biol.* 64:480–491.
34. Schibler, M. J., and J. D. Pickett-Heaps. 1980. Mitosis in Oedogonuim: spindle microfilaments and the origin of the kinetochore fiber. *Eur. J. Cell Biol.* 22:687–698.
35. Sluder, G., and C. L. Reider. 1985. Experimental separation of pronucleii in fertilized sea urchin eggs: chromosomes do not organize a spindle in the absence of centrosomes. *J. Cell Biol.* 100:897–903.
36. Snyder, J. A., and J. R. McIntosh. 1975. Initiation and growth of microtubules from mitotic centers in lysed mammalian cells. *J. Cell Biol.* 67:744–760.
37. Summers, K., and M. W. Kirschner. 1979. Characteristics of the polar assembly and disassembly of microtubules observed in vitro by darkfield light microscopy. *J. Cell Biol.* 83:205–217.
38. Telzer, B. R., M. J. Moses, and J. L. Rosenbaum. 1975. Assembly of microtubules onto kinetochores of isolated mitotic chromosomes of HeLa cells. *Proc. Natl. Acad. Sci. USA.* 72:4023–4027.
39. Witt, P. L., H. Ris, and G. G. Borisy. 1980 Origin of kinetochore microtubules in CHO cells. *Chromosoma (Berl.).* 81:483–505.
40. Witt, P. L., H. Ris, and G. G. Borisy. 1981. Structures of kinetochore fibers: microtubule continuity and intermicrotubule bridges. *Chromosoma (Berl.).* 83:523–540.